# Maskless Grayscale Lithography Using a Positive-Tone Photodefinable Polyimide for MEMS Applications

Joseph H. Lake, Scott D. Cambron, Kevin M. Walsh, and Shamus McNamara

***Abstract*—The novel use of a positive-tone photosensitive polyimide for the rapid production of grayscale features using a maskless lithography system is demonstrated. The removal rate of the polyimide, HD-8820, is characterized as a function of exposure dose. A broad contrast curve is found that is suitable for grayscale lithography. Three-dimensional polyimide structures up to 22 $\mu$m thick are demonstrated, and the surface roughness after the final cure is $Ra = 4.4$ nm, which is suitable for many microelectromechanical systems (MEMS) applications, including many optical applications. Tensile testing of 63 polyimide samples shows excellent mechanical properties for four different polyimide thicknesses produced with grayscale lithography. The modulus of elasticity is found to be 1.92 GPa, the yield strength to be 103 MPa, the fracture strength to be 133 MPa, and the percent elongation to be 51%. The test results show that the mechanical properties are consistent and do not change due to a partial exposure to UV light. The entire fabrication sequence, from computer-aided design file to cured structure, can be performed in less than 4 h, making this a fast low-cost method of producing polymer MEMS devices with excellent mechanical properties. [2011-0085]**

***Index Terms*—Grayscale lithography, microelectromechanical systems (MEMS), photodefinable polyimide, photolithography, polyimide.**

## I. Introduction

GRAYSCALE lithography is a technique that is used to overcome the 2-D limitation of traditional photolithography by varying the photoresist dose so that, during the development step, a 3-D structure results. Some examples of devices that benefit from a true 3-D structure include lenses [1], gratings [2], microfluidic channels [3], and photonic crystals [4]. Because development occurs first at the surface of the exposed film, a positive-tone photoresist is often preferred over a negative-tone photoresist for grayscale lithography. It is possible to create grayscale masks that may be used in a conventional mask aligner, such as by using subwavelength dithering [3], e-beam exposure of a high-energy-beam-sensitive glass [5], dyed polymers with varying thickness [6], or laser-induced oxidation of metallic films [7]. Most grayscale masks are expensive to fabricate, making them less attractive for applications in which frequent revisions may be necessary, small quantities are required, or for prototyping. However, grayscale masks can be quite attractive when used for the production of large numbers of devices. An alternative method of varying the photoresist dose is to directly write the image using an e-beam writer [8] or a laser pattern generator. Although useful for prototyping, the associated long write times make this technique unattractive for manufacturing. In this paper, a direct-write technique using a deformable mirror device (DMD)-based maskless lithography system is demonstrated that simultaneously images an entire die with any desired pattern. This technique does not have as high a resolution as the other techniques, but this is a limitation of the equipment used, not a fundamental limitation of the technique being presented.

Normally microelectromechanical systems (MEMS) devices are designed to operate for many years. Thus, the materials used must have long-term mechanical stability. Unfortunately, typical photoresists do not have long-term mechanical stability and are thus only suitable as an image transfer layer for a layer to be etched underneath. Polyimide is a popular material because of its excellent properties [9]–[12], but most photodefinable polyimides do not have good mechanical characteristics. The grayscale characteristics of HD-8820, which is a positive-tone photodefinable polyimide from HD Microsystems, were investigated in [13] for subsequent graphitization, but the mechanical properties of the polyimide were not investigated. Although the technical data sheet [14] may be consulted to find the nominal mechanical properties, the effects of a partial exposure during grayscale lithography on the mechanical properties were not known. The mechanical properties of HD-8820 are investigated in this paper.

When a polymer material is exposed to high-energy radiation, such as UV light, chemical changes such as scission events or cross-linking events may occur. Often both events occur simultaneously. These chemical changes may alter the mechanical properties, such as the degradation of polymethylmethacrylate or other polymers when exposed to UV light [15]. The Young's modulus of SU-8 has been reported to depend on the UV exposure dose [16]. Fully cured polyimide films are only slightly affected by UV radiation [17], but the effects

Manuscript received March 20, 2011; revised July 25, 2011; accepted July 26, 2011. Date of publication October 3, 2011; date of current version December 2, 2011. This work was supported by the U.S. Navy under Contract DAAB07-03-D-B010/TO-0198. Subject Editor C. H. Ahn.

J. H. Lake, K. M. Walsh, and S. McNamara are with the Department of Electrical and Computer Engineering, University of Louisville, Louisville, KY 40292 USA (e-mail: joseph.lake@louisville.edu; kmwals01@gwise.louisville.edu; shamus.mcnamara@louisville.edu).

S. D. Cambron is with the Bioengineering Department, University of Louisville, Louisville, KY 40292 USA (e-mail: sdcamb01@gwise.louisville.edu).

Color versions of one or more of the figures in this paper are available online at http://ieeexplore.ieee.org.

Digital Object Identifier 10.1109/JMEMS.2011.2167664

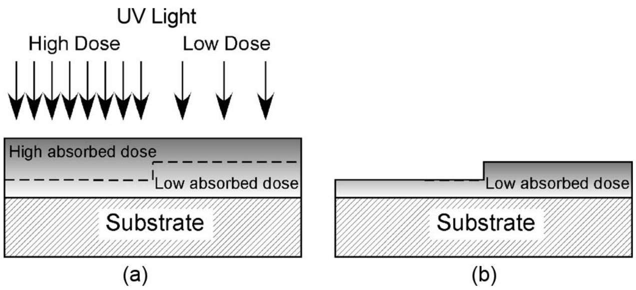


Fig. 1. (a) Schematic of a positive photoresist exposed to a high dose and a low dose for grayscale lithography. (b) Resulting photoresist profile after development.

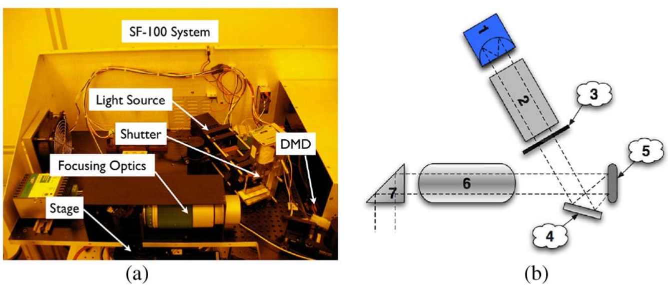


Fig. 2. (a) Layout of SF-100 DMD-based maskless lithography system used for grayscale exposures. (b) Schematic of the DMD-based maskless lithography system. Light from (1) the mercury lamp passes through (2) collimating optics and (3) a shutter. After reflecting off (4) a mirror, the light is reflected off (5) the smart filter, which contains the DMD array. Finally, the light goes through (6) the imaging optics and is reflected off (7) a mirror to the substrate on the stage below the optics.

of UV radiation on polyimide prior to imidization are not as well characterized because there are many chemistries in use. In grayscale lithography with positive photoresists, a region is exposed to a specific exposure dose, causing chemical and potentially mechanical changes to occur to the organic material. The absorbed dose is the largest at the top of the photoresist, and the dose decreases with penetration depth, as shown in Fig. 1. During development, the top portion of the photoresist, which has been exposed to a larger dose, is removed, while the lower portion of the photoresist, which has been exposed to a smaller dose, remains adhered to the substrate. The final structure consists of photoresist that has been exposed to UV light, and thus, it is desirable to determine whether the mechanical properties of the final photoresist have been affected. This paper investigates the mechanical properties of the final HD-8820 structure after exposure to varying levels of UV light during the grayscale exposure step.

Building upon results presented at a conference [18], this paper will address aspects of three current limitations to grayscale lithography: 1) cost; 2) throughput; and 3) a good photodefinable polymer. The cost and throughput are addressed through the use of a direct-write technique using an Intelligent Micro Patterning Systems SF-100 maskless exposure system that eliminates the cost of a grayscale photomask and overcomes the throughput issues with serial write lithography. The good photodefinable polymer issue is addressed through the use of HD-8820 polyimide. The grayscale and mechanical properties of the HD-8820 are investigated.

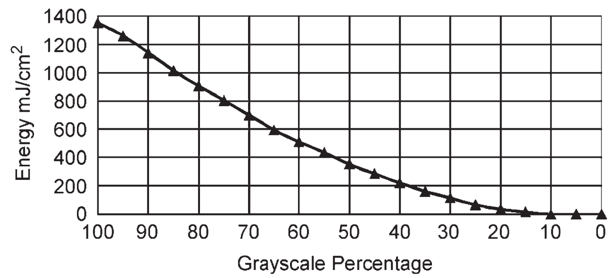


Fig. 3. Measured light output from the SF-100 as a function of the input grayscale percentage, integrated over a 10-s exposure. Both the $i$-line (365 nm) and $h$-line (405 nm) were measured. White corresponds to 100%, and black corresponds to 0%.

## II. GRAYSCALE LITHOGRAPHY

The SF-100 DMD-based maskless lithography system from Intelligent Micro Patterning Systems is used to perform the grayscale lithography (Fig. 2). This system accepts standard 32-b bitmap files as input, allowing designs to be generated using many standard graphics, desktop publishing, or computer-aided design (CAD) packages. The designs presented in this paper were generated using Omnigraffle running under Mac OS 10.5.5 using a 15 mm $\times$ 13 mm canvas. This canvas size corresponds to the frame size of the SF-100. Multiple frames can be used and stitched together to form larger structures. The design was then exported as a 1680-dpi Tagged Image File Format (TIFF) file; at this resolution, there is a 1:1 correlation between the drawn pixels and the mirrors in the DMD array. AutoVue was then used to convert the TIFF file format to the bitmap file format required by the lithography system.

The DMD system was characterized by measuring the energy output as a function of the input percentage. Fig. 3 shows the total measured energy for $h$- and $i$-line wavelengths measured at 5% increments with 100% being white and 0% representing black. This figure shows that the light output is not linear with respect to grayscale percentage. This is important to note because of its impact on changing the exposure time. For example, the exposure dose at 100% grayscale for a 10-s exposure (1380 mJ/cm$^2$) does not equal the exposure dose at 50% grayscale for a 20-s exposure (1100 mJ/cm$^2$). An equation that fits the data is

$$y = 0.1393x^2 + 0.0353x.$$

The following procedure was used to create grayscale structures made of polyimide films. The polyimide HD-8820 was spun on a wafer with a thickness ranging from approximately 4 to 24 $\mu$m, adjustable by changing the spin speed. After spinning, the films were soft baked on a hot plate in an air atmosphere at 123 °C for 3 min. These films were then exposed using the SF-100 system using a 10-s exposure. Initial attempts at pan development resulted in damage to unexposed areas of the polyimide film, so a spin development recipe was developed (Table I). After developing, the wafer was rinsed with deionized water and spun dry. The film was cured using a hot plate with controllable ramp and $N_2$ blanket to minimize oxidation during the high temperature cure. The final cure was performed in two stages: ramping from room temperature to 200 °C at 4 °C/min

TABLE I
SPIN DEVELOPMENT RECIPE USED FOR GRAYSCALE EXPOSED HD-8820 FILMS. THIS RECIPE IS REPEATED FOUR TIMES FOR A 20-$\mu$m NOMINAL THICKNESS

| Speed (RPM) | Time (seconds) | Chemical Spray |
|---|---|---|
| 1000 | 3 | MF-319 |
| 50 | 3 | MF-319 |
| 0 | 40 | None |

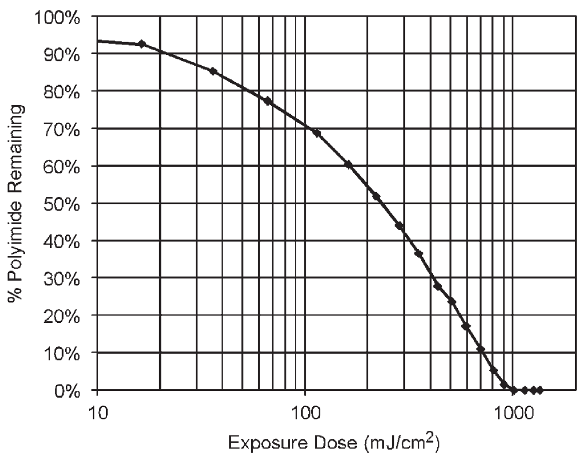


Fig. 4. This graph shows the percentage of polyimide that remained after the development step as a function of the total exposure dose.

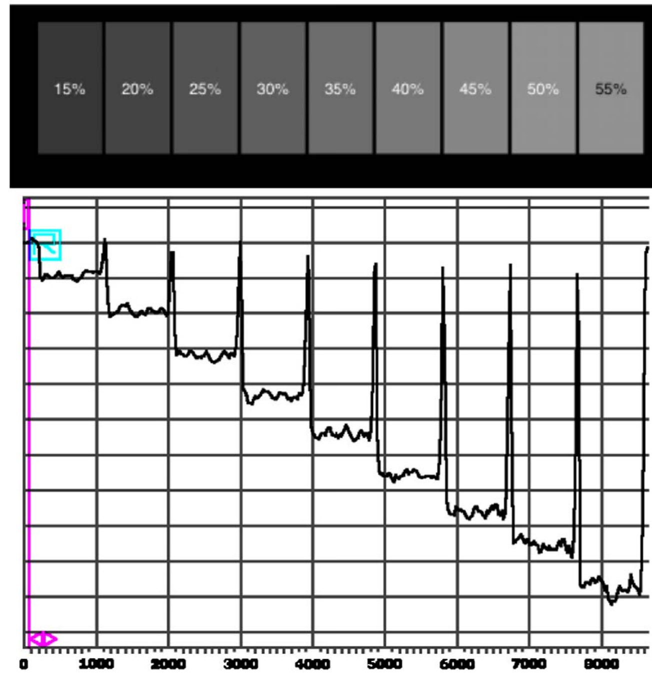


Fig. 5. (Top) Bitmap file used to characterize the grayscale lithography process. (Bottom) Contact profilometer line scan of the developed HD-8820 film, after exposure to the bitmap file shown above, but before the final cure. The peaks in the profilometer scan are due to (black lines in the bitmap file) the unexposed regions separating the regions with different grayscale levels.

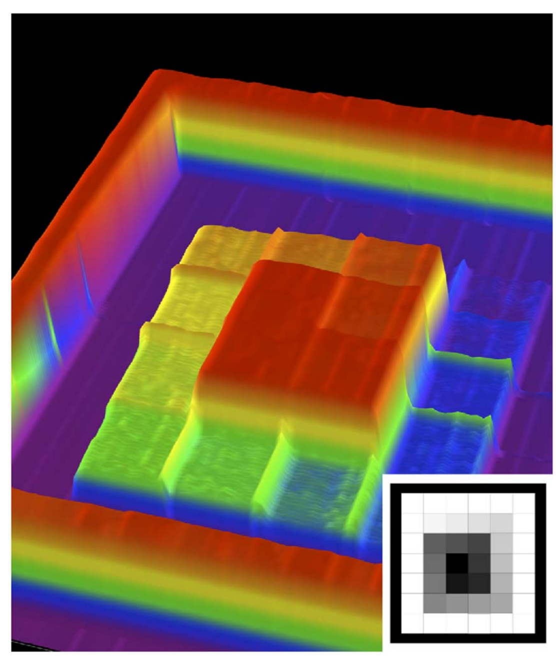

Fig. 6. Three-dimensional profile of a developed HD-8820 staircase structure measured with a Veeco Dektak contact profilometer. The (inset) grayscale pattern is composed of 300 $\mu$m $\times$ 300 $\mu$m squares spiraling from (black) 0% in the center to (white) 100% in 5% steps. The overall film thickness for this film sample is 22.5 $\mu$m. The bumps between the steps are due to unexposed regions (one pixel wide black lines in the bitmap file) with a width of 15 $\mu$m.

with a 30-min soak and from 200 °C to 350 °C at 2.5 °C/min with a 60-min soak. The hot plate was then allowed to cool to room temperature while maintaining the $N_2$ blanket.

The development rate of the HD-8820 was studied. Fig. 4 shows the percent polyimide remaining as a function of exposure dose for a 24-$\mu$m-thick polyimide film. The broad contrast curve $(\gamma = 0.8)$ is beneficial for producing grayscale structures. Fig. 5 shows an example of the thickness profile obtained as a function of grayscale percentage for a 10-s exposure. The top portion of the figure shows the bitmap file used. The bottom portion of the figure shows the measured profile obtained after development, but before final curing, obtained using a Veeco Dektak profilometer.

Fig. 6 shows an example of a structure that may be generated using this grayscale lithography process. The pixel size used to produce the structures shown in the figure is 15 $\mu$m by 15 $\mu$m. Each step is 300 $\mu$m by 300 $\mu$m (20 pixels by 20 pixels). The maximum thickness of the polyimide is 22.5 $\mu$m. The inset shows the grayscale bitmap mask file that was used to create the pattern in the polyimide. Each step represents a 5% change in the grayscale value used in the bitmap mask file. The bump separating each step is due to a single pixel wide line in the bitmap file. These bumps may be eliminated by eliminating the black line.

The surface roughness was measured after development [Fig. 7(a)] and after the final cure [Fig. 7(b)]. The peaks shown in Fig. 7(a) correspond to the individual micromirrors in the DMD's array. The peak-to-peak distance of 15 $\mu$m matches the pixel size of the exposure system. The surface roughness $Ra$ was measured to be 11.2 nm immediately after development. This roughness improved greatly after the final cure of the polyimide [Fig. 7(b)]. The fully cured polyimide film had a surface roughness $Ra$ of 4.4 nm. The final surface roughness

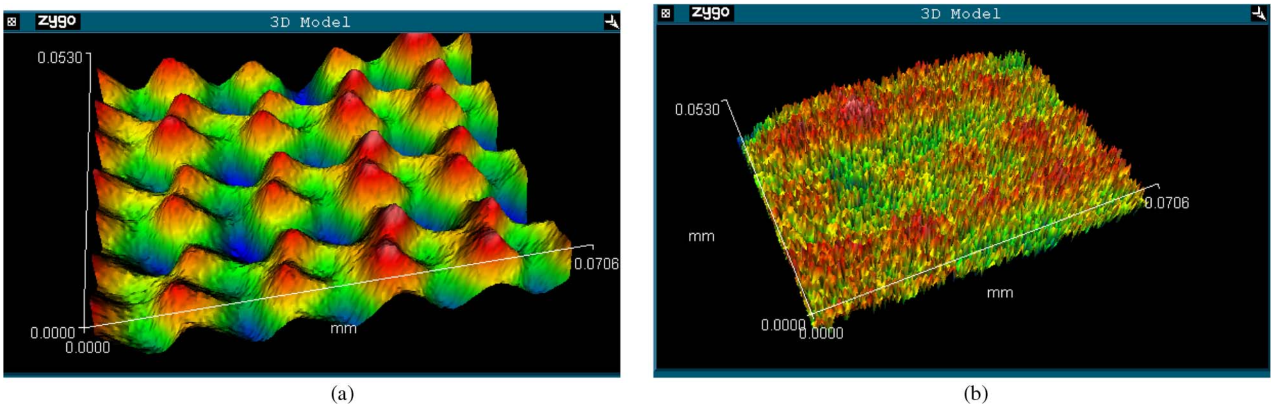


Fig. 7. Three-dimensional profile of surface roughness of the polyimide, measured with a Zygo white light interferometer. (a) Prior to the final cure, peaks with a spacing of 15 $\mu$m are observed, corresponding to the individual micromirrors in the DMD array. The surface roughness $Ra$ is 11.2 nm. (b) After the final cure, the large peaks that were present before the cure have nearly been eliminated. The surface roughness $Ra$ is reduced to 4.4 nm.

makes this polymer suitable for many MEMS applications, including many optical device applications.

## III. Mechanical Properties

The process of creating grayscale structures involves partially exposing the polyimide to UV light and removing portions of the polyimide during the development step. The polyimide that remains on the wafer has been partially exposed and potentially been altered from its unexposed state. The mechanical properties of polyimide of various thicknesses as well as polyimide that is unexposed were investigated to determine the effects of the grayscale lithography process on the polyimide.

Rectangular bands of polyimide were formed using grayscale lithography and peeled off a silicon wafer. It is relatively easy to peel the polyimide off the wafer when no adhesion promoter is used. The sample groups used were 17-$\mu$m-thick unexposed polyimide, 15.5-$\mu$m-thick exposed polyimide, 7.5-$\mu$m-thick exposed polyimide, and 4.5-$\mu$m-thick exposed polyimide. The polyimide strips were all 6 mm wide and 24.7 mm long. Fig. 8 shows a strip of polyimide in an RSA III Rheometrics System Analyzer (TA Instruments, New Castle, DE). A 0.25-in-wide single-sided Kapton tape, applied to both ends and sides of the samples, is used at the grippers for strain relief. Half of the samples were tested at a strain rate of 0.3 microstrain per second, and the other half of the samples were tested at a strain rate of 0.6 microstrain per second. The typical test time was 3000 s (50 min). The distribution of samples measured was 16 samples that are 17-$\mu$m-thick polyimide, 18 samples that are 15.5 $\mu$m, 13 samples that are 7.5 $\mu$m, and 16 samples that are 4.5 $\mu$m.

The averages of the measured modulus of elasticity, yield stress, fracture stress, and percent elongation are shown in Fig. 9. The modulus of elasticity and the yield strength are nearly the same for all four thicknesses. The fracture strength and the percent elongation at break are also similar in values for all four thicknesses, although these two measurements show much greater variation. For the fracture strength and percent elongation, the standard deviation increases as the sample gets thinner. This is attributed to the fact that sheet buckling was more likely to occur during tensile testing for the thinner samples. It was also observed that, despite the nitrogen curtain used for the polyimide cure, portions of the wafer would be partially oxidized, as determined by a brownish discoloration. The discolored samples were observed to be slightly more brittle.

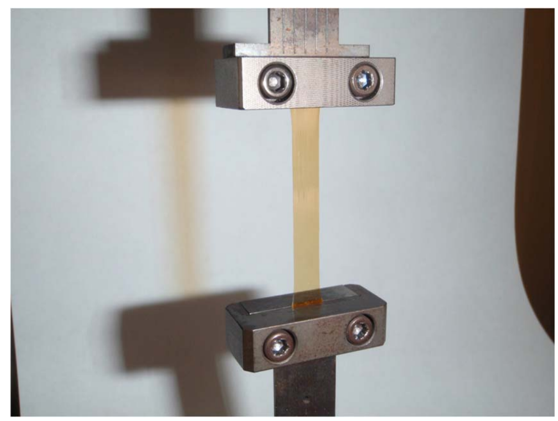

Fig. 8. Photograph of strip of polyimide undergoing tensile testing.

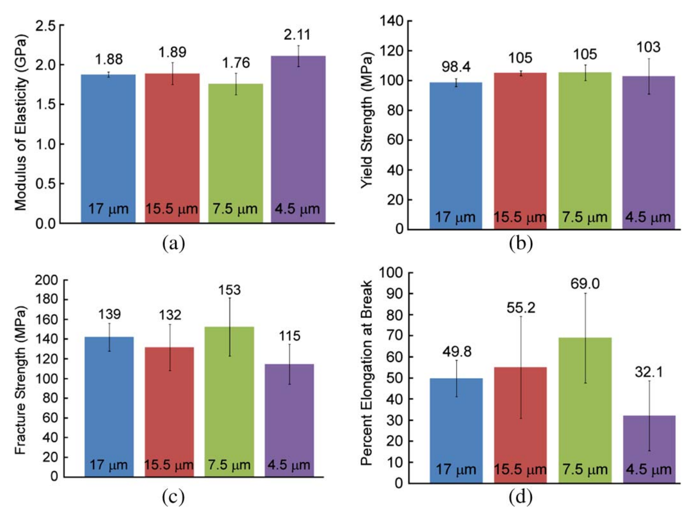


Fig. 9. Comparison of the averages of (a) the modulus of elasticity, (b) the yield strength, (c) the fracture strength, and (d) the percent elongation at break for polyimide samples of thicknesses 17, 15.5, 7.5, and 4.5 $\mu$m.

Averaging the results from all the samples, regardless of thickness, the modulus of elasticity is found to be 1.92 GPa, the yield strength to be 103 MPa, the fracture strength to be 133 MPa, and the percent elongation to be 51%. An exact comparison cannot be made between these results and the values listed on the manufacturer's data sheet for the polyimide because the processing conditions are not identical, but a comparison is still useful. On the manufacturer's data sheet is an entry for a 350 °C cure on a hot plate with an "air atmosphere" and an entry for a 350 °C cure in nitrogen in a furnace, with reported Young's modulus values of 2.6 and 2.0 GPa, respectively. The method reported here used a hot plate with a nitrogen atmosphere, which is a combination of those two approaches. It may be noted that 1.9 GPa is almost the same as 2.0 GPa, which indicates a cure in a nitrogen atmosphere may result in a lower Young's modulus than a cure with oxygen present.

## IV. Conclusion

Maskless grayscale lithography using the positive-tone polyimide HD-8820 was successfully performed using an SF-100 DMD-based maskless lithography system from Intelligent Micro Patterning Systems. Nonlinearities in the exposure dose from the SF-100 were documented, and the amount of polyimide that is removed during the development step was characterized as a function of exposure dose. The entire process, from CAD file to final structure, took less than 4 h to complete and did not require an expensive grayscale photomask, making this an attractive process for manufacturing MEMS devices.

It was found that, after exposure and developing, there is a significant amount of roughness due to the edges of the micromirror array used in the SF-100 to create the pattern. After curing the sample, the roughness is significantly reduced, resulting in a $Ra$ of 4.4 nm. This roughness is adequate for many MEMS applications, including many optical applications.

In all, 63 polyimide strips with four different thicknesses were fabricated and underwent tensile testing. The samples ranged from 17 $\mu$m thick, which underwent no UV exposure, to just 4.5 $\mu$m thick, which required a substantial UV exposure to remove the upper 12.5 $\mu$m of polyimide. The modulus of elasticity, yield strength, fracture strength, and percent elongation were all measured, and it was found that the thickness of polyimide, and thus the amount of exposure to UV light, had little or no effect on the polyimide mechanical properties. The average modulus of elasticity is found to be 1.92 GPa, the average yield strength to be 103 MPa, the average fracture strength to be 133 MPa, and the average percent elongation to be 51%. The good mechanical properties that were measured, as well as the fact that the mechanical properties do not change with thickness, make the HD-8820 polyimide an attractive material for use in grayscale lithography.

## Acknowledgment

The technical program oversight was provided by the Naval Surface Warfare Center, Crane Division.

## References

[1] C. Rooman, M. Kuijk, R. Vounckx, and P. Heremans, "Reflective–refractive microlens for efficient light-emitting-diode-to-fiber coupling," *Opt. Eng.*, vol. 44, no. 9, p. 95 005, Sep. 2005.
[2] U. Levy, B. Desiatov, I. Goykhman, T. Nachmias, A. Ohayon, and S. E. Meltzer, "Design, fabrication, and characterization of circular Dammann gratings based on grayscale lithography," *Opt. Lett.*, vol. 35, no. 6, pp. 880–882, Mar. 2010.
[3] V. Nock and R. J. Blaikie, "Fabrication of optical grayscale masks for tapered microfluidic devices," *Microelectron. Eng.*, vol. 85, no. 5/6, pp. 1077–1082, May/Jun. 2008.
[4] D. W. Prather, J. Murakowski, S. Venkataraman, P. Yao, A. Balcha, T. Dillon, and D. Pustai, "Novel fabrication methods for 2D photonic crystals in silicon slab waveguides," in *Proc. SPIE, Micromachining Technology for Micro-Optics and Nano-Optics*, 2003, vol. 4984, pp. 89–99.
[5] W. Daschner, P. Long, R. Stein, C. Wu, and S. H. Lee, "General aspheric refractive micro-optics fabricated by optical lithography using a high energy beam sensitive glass gray-level mask," *J. Vac. Sci. Technol. B, Microelectron. Nanometer Struct.*, vol. 14, no. 6, pp. 3730–3733, Nov. 1996.
[6] N. S. Korivi, Y. X. Zhou, and L. Jiang, "Grayscale lithography by a polymer photomask doped with laser dye," *J. Vac. Sci. Technol. B, Microelectron. Nanometer Struct.*, vol. 26, no. 1, pp. 62–66, Jan. 2008.
[7] C. F. Guo, S. Cao, P. Jiang, Y. Fang, J. Zhang, Y. Fan, Y. Wang, W. Xu, Z. Zhao, and Q. Liu, "Grayscale photomask fabricated by laser direct writing in metallic nano-films," *Opt. Exp.*, vol. 17, no. 22, pp. 19 981–19 987, Oct. 2009.
[8] S. Y. Lee and K. Anbumony, "Accurate control of remaining resist depth for nanoscale three-dimensional structures in electron-beam grayscale lithography," *J. Vac. Sci. Technol. B, Microelectron. Nanometer Struct.*, vol. 25, no. 6, pp. 2008–2012, Nov. 2007.
[9] M. Martin, M. Crain, K. Walsh, R. A. McGill, E. Houser, J. Stepnowski, S. Stepnowski, W. Huey-Daw, and S. Ross, "Microfabricated vapor preconcentrator for portable ion mobility spectroscopy," *Sens. Actuators B, Chem.*, vol. 126, no. 2, pp. 447–454, 2007.
[10] J. M. Zara, P. Mills, and P. Patterson, "Polyimide MEMS Actuators for Medical Imaging," in *Proc. SPIE Conf. MOEMS Display Imag. Syst.*, 2005, pp. 93–103.
[11] C. Shearwood, M. A. Harradine, T. S. Birch, and J. C. Stevens, "Applications of polyimide membranes to MEMS technology [hearing aid microspeaker]," *Microelectron. Eng.*, vol. 30, no. 1–4, pp. 547–550, Jan. 1996.
[12] M. Topper, T. Fischer, T. Baumgartner, and H. Reichl, "A comparison of thin film polymers for wafer level packaging," in *Proc. IEEE Elecron. Compon. Technol. Conf.*, Las Vegas, NV, 2010, pp. 769–776.
[13] S. Akbar, E. Imhoff, and F. Kub, "Gray-scale lithography of photosensitive polyimide and its graphitization," in *Proc. SPIE, Advances in Resist Materials and Processing Technology XXIV*, 2007, vol. 6519, pp. 65 191I-1–65 191I-12.
[14] *HD MicroSystems Product Selection Guide*, HD MicroSystems, Parlin, NJ, Sep. 2008.
[15] N. Nagai, T. Matsunobe, and T. Imai, "Infrared analysis of depth profiles in UV-photochemical degradation of polymers," *Polym. Degradation Stability*, vol. 88, no. 2, pp. 224–233, May 2005.
[16] R. Feng and R. J. Farris, "Influence of processing conditions on the thermal and mechanical properties of SU8 negative photoresist coatings," *J. Micromech. Microeng.*, vol. 13, no. 1, pp. 80–88, Jan. 2003.
[17] K. Rasmussen, G. Grampp, M. van Eesbeek, and T. Rohr, "Thermal and UV degradation of polymer films studied *in situ* with ESR spectroscopy," *ACS Appl. Mater. Interf.*, vol. 2, no. 7, pp. 1879–1883, Jul. 2010.
[18] J. Lake, K. Walsh, and S. McNamara, "Low-cost maskless grayscale lithography using a new photodefinable polyimide for polymer MEMS applications," in *Proc. Int. Solid-State Sens. Actuators, Microsyst. Conf. (Transducers)*, Denver, CO, 2009, pp. 1889–1891.

**Joseph H. Lake** received the B.S. and M.S. degrees in electrical and computer engineering from the University of Louisville, Louisville, KY, in 2003 and 2006, respectively.

He is currently a Research Engineer with the Department of Electrical and Computer Engineering, University of Louisville, and works in the Micro/Nano Technology Center. His research interests are microfabrication and microelectromechanical systems processing.

**Scott D. Cambron** received the B.S. and M.Eng. degrees from the University of Louisville, Louisville, KY, in 2004 and 2007, respectively, where he is currently working toward the Ph.D. degree in mechanical engineering.

He is currently a Research Engineer with the Bioengineering Department, University of Louisville. His research interests include trace explosive detection and micromachining/manufacturing techniques.

**Kevin M. Walsh** received the B.S. and M.Eng. degrees in electrical engineering from the University of Louisville (UofL), Louisville, KY, in 1978 and 1985, respectively, and the Ph.D. degree in electrical engineering (microelectronics) from the University of Cincinnati, Cincinnati, OH, in 1992.

He is currently the Fife Endowed Professor of Electrical and Computer Engineering at the University of Louisville, where he also serves as the Founding Director of the UofL Micro/Nano Technology Center and its associated 10 000 $ft^2$ class 100 cleanroom facility. He is the holder of seven patents and is the Cofounder of three technical start-up companies. He has taught over 20 different courses, advised over 25 completed theses, and published over 100 technical papers in the areas of micro-/nanotechnology, microelectromechanical systems, microfabrication, packaging, sensors, actuators, cleanroom design/operation, and micro-/nanotechnology course development.

Prof. Walsh was inducted into the Trinity High School Hall of Fame in 2000, into the UofL Athletic Hall of Fame in 2001, and the Kentucky Tennis Hall of Fame in 2005.

**Shamus McNamara** received the B.S. and M.S. degrees in electrical engineering from Rensselaer Polytechnic Institute, Troy, NY, in 1994 and 1996, respectively, and the Ph.D. degree in electrical engineering from the University of Wisconsin, Madison, in 2002.

He did his postdoctoral work at the University of Michigan, Ann Arbor, and is the Cofounder of a start-up company. He is currently an Assistant Professor in the Department of Electrical and Computer Engineering, University of Louisville, Louisville, KY, where he is also the Associate Director of the Micro/Nano Technology Center. His research interests lie in the fields of microfabrication and microelectromechanical systems.